Proceedings Ninth Workshop Geothermal Reservoir Engineering
Stanford University, Stanford, California, December 1983
SGP-TR-74

RESERVOIR SIMULATION ON THE CERRO PRIETO GEOTHERMAL FIELD: A CONTINUING STUDY.

*M. Castañeda, **R. Márquez, *V. Arellano, **C.A. Esquer

*Instituto de Investigaciones Eléctricas
**Coordinadora Ejecutiva de Cerro Prieto
Mexicali, B.C., Mexico

INTRODUCTION

The Cerro Prieto geothermal field is a liquid-dominated geothermal reservoir of complex geological and hydrological structure. It is located at the southern end of the Salton-Mexicali trough which includes other geothermal annomalies as Heber and East Mesa. Although in 1973, the initial power plant installed capacity was 75 MW of electrical power, this amount increased to 180 MW in 1981 as field development continued. It is expected to have a generating capacity of 620 MW by the end of 1985, when two new plants will be completely in operation. Questions about field deliverability, reservoir life and ultimate recovery related to planned installations are being presently asked. Numerical modeling studies can give very valuable answers to these questions, even at the early stages in the development of a field.

An effort to simulate the Cerro Prieto geothermal reservoir has been undergoing for almost two years. A joint project among Comision Federal de Electricidad (CFE), Instituto de Investigaciones Electricas (IIE) and Intercomp of Houston, Texas, was created to perform reservoir engineering and simulation studies on this field. The final project objective is to simulate the behaviour of the old field region when production from additional wells located in the undeveloped field zones will be used for feeding the new power plants.

Early project results from a preliminary material balance applied to the old part of this field (Cerro Prieto I region) using a simplified geological model had indicated the existance of a strong cold water recharge into this region (Castañeda et. al., 1982). This conclusion agreed with the results presented by previous authors (Westwood, 1981; Grant, 1982; Bermejo, 1979).

Now, a tridimensional coarse grid reservoir model has been extended over the entire field as additional reservoir information has been generated and become available to this project. This study presents the simulation efforts to obtain a reservoir pressure and enthalpy history match of the Cerro Prieto I region, using this coarse grid model, when production from other field regions is taken into account. The influence of some reservoir features (i.e., geologic faults) on these match as well as predictive calculations are also presented.

RESERVOIR MODEL

The extended field area used in this simulation study is presented in figure 1. This area (19.5 Km^2) encloses the practical boundaries of the field, as they were defined by CFE[11].

The tridimensional coarse grid model imposed to this area was based on the geologic model presented by Cobo, 1981. Basing his model on well cuttings, he recognized five lithologic units within this area that showed differences in origin, mineralogy, grading, color, etc. From the oldest to most recent, these lithologic units are: biotite granite, gray shale, coffe-colored shale, mudstone and unconsolidated sediments. Most all Cerro Prieto wells are completed on the gray shale and/or coffe-colored shale units although there are some wells that have reached the granitic basement (Sánchez and De la Peña, 1981).

Although this geologic model replaced the one we had been using in the preliminary material balance calculation of this project (a model based on well logs interpretation, (Abril 1978), they showed some similarities on both proposed lithologic columns. Cobo's mineralogic model was then used mainly because there was not enough reservoir information in the other model to characterize the extended field area.

Figure 2 presents a tridimensional representation of Cobo's contour map of the top of the gray shale unit. This figure clearly suggests that the field area of study can be subdivided in 5 main blocks (blocks I through V) limited by the respective faults. This figure also suggests that hotter reservoir zones are expected to be found deeper in the southeast part of the field (Cerro Prieto II area) as it has been indicated by other authors and confirmed by drilling (Domínguez, 1982, Rivera et. al., 1982).

For simulation purposes, these five irregular blocks were replaced by rectangular blocks but the same respective block area was kept. Figure 3 shows this schematic representation.

Faults were included in this representation by assigning to them a defined dimension (thickness of 50 m). For this study, Hidalgo and Patzcuaro faults were considered only.

Figure 4 shows the model vertical representation. Mainly, each block consists of 4 units: 1) a cooler aquifer (unconsolidated sediments) overlying the main geothermal reservoir, 2) a shaly layer (Cobo's mudstone layer and sometimes referred as a "cap rock" by other authors), 3) a shaly sand layer (gray shale coffe-colored shale units), considered as the zone of geothermal interest (higher temperature and higher permeability zone, and 4) the granitic basement. The thickness of each unit represents an average value for each block. Cobo's contour maps of each unit were used for such purpose.

The geologic faults were only included in the gray shale_coffe-colored shale unit. Both faults were sealed at the mudstone layer and they did not continue through the unconsolidated sediments.

FORMATION PROPERTIES

For this study, the rock properties were determined by means of geophysical well log analysis and well test data (Castañeda et. al., 1982). This rather scarce data was not sufficient to define the entire area of study or to characterize all lithologic units. Some rock properties were inferred or assumed in zones where no information was available. Figure 5 presents the assigned reservoir parameters to all units.

INITIAL CONDITIONS

The initial field temperature distribution used in this work is presented in figure 6. These temperature profiles were obtained from isoterm maps elaborated from shut-in wells temperature data (Castañeda et. al., 1983). However, the temperature distribution of the eastern part of the field may have been affected by former explotation of the western area. Thus, the presented temperature profiles for the part of the field (blocks 3, 4, and 5) were only used as an approximation to the real initial temperature values.

The initial pressure distribution was computed by assuming an atmospheric pressure at the ground surface and then calculating a hydrostatic distribution of pressure with depth, subject to the initial temperature distribution. These initial conditions neglect any changes that might have occurred in the western field area before 1973. Although some wells were completed and tested in this area on the late 60's, full production started in 1973.

The initial conditions imply that the reservoir was at single phase (liquid) condition prior to production at Cerro Prieto. It has been indicated by some authors (Grant et. al. 1981) that although there was a region of boiling fluid initially in the reservoir, this region was local and very small and that most of reservoir rock contained fluid at single phase (liquid). If that condition of boiling existed in the reservoir, this was a local phenomeno and could not be represented in our coarse grid model.

BOUNDARY CONDITIONS

Presently, the fact that a strong recharge is taking place at the old part of the field (Cerro Prieto I region) is generally well accepted although there has been no agreement on the magnitude and direction of such recharge. Some authors (Bermejo, 1979; Sánchez and De la Peña, 1981) have suggested that there is a significant recharge into this region from the north and east. Others (Grant et. al., 1981; Lippman and Bodvarsson, 1982) have found that the most of the recharge comes from the west and shallower zones.

In this study, a steady-state recharge representation was selected. This required placing aquifer blocks (outer elements) to the rectangular grid model. Aquifer blocks are defined as those elements in the model that communicate directly with an aquifer that is not itself modeled as part of the calculation grid but whose effects are introduced through the specific aquifer terms. The influx into an aquifer block is calculated as:

$$\text{influx rate} = VAB \times (P_i - P_{n+1}) \text{ RB water/day}$$

where:

P_i = initial block pressure

P_{n+1} = block pressure at end of time step

VAB = aquifer influx coefficient RB/DAY/psi

The aquifer blocks in the model are: in the western side of the model, nodes I=1, J=1 to 7; in the northern side, J=1, I=1 to 4; in the eastern side, I=4, J=1 to 7 (in all three sides, layers K=1 to 18). In the southern side, no recharge was considered.

Initial temperature profiles of periphery wells were used to represent the recharge temperature. For the western side of the model, well M-6 (block I), well Q-743 (block II), well M-92 (block IV) and well M-189 (block V) were used for such purpose. Well M-94 (blocks I and III) was considered for the northern side. For the eastern side, well H-2 (block III) and well NL-1 (blocks IV and V). Figure 7 shows these profiles.

SIMULATION RUNS

Intercomp's geothermal reservoir simulator GEOTHERM) was used in this work. The finite difference formulation of this simulator is explained by Coats, 1974. This simulator does not account for the presence of inert gases or for varying concentration and precipitation of dissolved solids.

The grid model representation including main blocks, layers, faults as well as aquifer blocks gave a total of 504 elements.

Rather than simulating a single well, groups of wells were formed according to their location in the field (at a given main block) and their depths of open intervals. In the latter case, the open intervals of each well were projected onto the model vertical representation. This procedure determined the producing layers of the model. Figure 8 shows the 17 groups of wells formed in this manner and their location in the grid model. Some of these wells are not presently on production and they are not accounted for in the histoy match process. They are wells needed for the two new power plants and will become producers in the predictive calculations.

Production history was taken from the monthly production data reported by CFE. Figures 9, 10 and 11 show the production assigned to each well in the model for blocks I, II and some wells in block III, respectively, during the production period of March 1973-May 1983.

The prime objective was to match the observed Cerro Prieto I (block I in the model) reservoir pressure and enthalpy history under the steady-state recharge assumption. These histories are presented in figure 12 and 13, respectively. Both histories are representative of a 1200 m depth zone. The histories suggest that this region has remained single phase (liquid) during this production period (at least until 1979). Some authors (Grant et. al., 1981); Lippman and Bodvarsson, 1982) have shown that although local near-well boiling is a common phenomenon in Cerro Prieto, a more extensive steam zone has not been formed in this part of the field, under exploitation conditions.

HISTORY MATCH RUNS

To handle the recharge strength, aquifer influx coefficients (VAB) were assigned to the aquifer blocks. The same recharge strength (i.e., same VAB values) were given to each of the three recharge sides of the model. This combination may not be unique and it is possible that an acceptable history match could also be obtained with any other combination. However, at this point, there is not enough field information in this coarse grid model to determine such combination exactly.

Because of the single phase (liquid) characteristic of this part of the reservoir during the history match period, the relative permeability concept was not relevant in this set of runs. However, if a two-phase zone develops in other field regions within the model during these runs, the same Corey's curves presented in reference 3 are used, but with residual liquid saturation of 0.3 and residual vapor saturation of 0.05.

For simulation studies, the single most important reservoir parameter is its permeability. Although rock porosity, compressibility, heat conductivity and heat capacity data are also needed for simulation studies, the effects of these parameters are not as great as those of permeability (Lippman and Bodvarsson, 1982). Therefore, the matching procedure was to vary the reservoir permeabilities in the production zones (gray shale-coffe-colored shale units) in combination with the variation of the aquifer influx coefficients. For sake of space, only the most representative simulation runs are presented here.

Figure 12 shows the simulated pressure when the initial reservoir parameters presented in figure 5 were used, for aquifer influx coefficients of 25, 100 and 300. In this case, k_h = 50 md and k_v = 10 md, for the production zone. As it can be observed, simulated pressures were higher than the observed values. To obtain a more gradual pressure drop throughout time, this rather low k_h/k_v ratio of 5 was increased to 10 (an acceptable ratio value for sedimentary reservoirs). Keeping the same k_h value, the vertical permeability (k_v) was reduced to 5 md. Figure 12 also shows this case when a VAB value of 200 is used. The respective simulated enthalpy is presented in figure 13.

Although a perfect pressure match was obtained for three of the four observed values, it was decided that the same weight should be given to the four observed points. An additional pressure drop could be obtained if the aquifer influx coefficients were reduced (i.e., less recharge) but this procedure would tend to decrease the cooling of that region (i.e., give higher simulated enthalpies) and the enthalpy match could not be obtained. Another method to produce an additional pressure drop could be by reducing the reservoir horizontal permeability and retarding the effect of the recharge on the reservoir pressure. To avoid an excessive pressure drop, the aquifer influx coefficient values have to be increased. Figure 14 presents both pressure and enthalpy matches when k_h was reduced to 30 md and a VAB of 1500 was used (the k_h/k_v of 10 was held constant).

It is interesting to notice that the simulator predicts an increase on reservoir pressure in the Cerro Prieto I region, after the period of 84 months (i.e., after 1979). Although no Cerro Prieto I isobaric maps have been made

after that period to verify this result, the above could be explained if we observe the production history of the wells # 2 and 3 on the model. These wells are directly responsible for the pressure drop in that zone (see figure 9). Though the mass flowrate of well 3 remains almost constant during this period, the mass flowrate of well 2 increases to a maximum and then it is reduced to almost half of that value after the period of 84 months. If this part of the field was being over-exploited, this mass flowrate reduction of well 2 should result in a pressure increase on that zone due to the strong aquifer recharge that is taking place in that region.

The rise in the observed enthalpy during the first two years could not be reproduced by this model. It is believed that such rise was produced by taking into account wells that were producing from an initial small two-phase region (Grant et. al., 1981). in the calculation of the overall enthalpy of Cerro Prieto I for those years.

The cooling of the region is due to recharge fluid of lower temperature coming from the west and north sides of the model, as well as that coming from blocks II and III at the same depth. Additional cooler fluid may be coming from the upper unconsolidated layer. Although the vertical permeability of the mudstone layer was set to 5 md (a considerably lower value than the reservoir permeability), some authors have shown that this value could not be sufficiently small to exclude significant downward flow through this layer (Grant et. al., 1981). However, with this coarse grid model, it is only possible to observe an overall effect of this recharge phenomenon.

EFFECT OF FAULTS

The trend of the Cerro Prieto I observed enthalpy in Figure 13 suggests that such enthalpy could stabilize after the 84 months period. To explore such possibility, the vertical permeability of the faults was increased to allow for mixing of more hot fluid from the lower hayers with cooler recharge fluids. The desired overall effect was to decrease the decline rate of the Cerro Prieto I temperature (i.e., enthalpy) at that depth. Although the faults vertical permeability was increased to 500, 1000 and even 10,000 md, the effect was insignificant to be noticed on the corresponding enthalpy graph.

PREDICTION OF FUTURE PERFORMANCE

A single prediction of future performance of the Cerro Prieto I region (i.e., after 1983) was performed. The calculation was merely an extension of the matched performance up through May of 1983. The simulator was allowed to run for an additional 20 years. Figure 15 presents the required mass flow rate to integrate the two new power plants, the wells that will become producers and the approximated dates of the plants starting operation (POISE, 1983). The mass flow rate of the already producing wells was held constant at the value reported by CFE in May of 1983.

Figure 16 shows the predicted pressure and enthalpy performance of this region. At the end of this period, the pressure has slowly decreased to 96 bars. The reservoir enthalpy has decreased to 1030 KJ/Kg, corresponding to a liquid water temperature value of 237°C.

The enthalpy decline is not lineal during this period. The rate of enthalpy decline diminishes with time and could possibly reach a constant enthalpy value for a longer period of time. As mentioned before, this phenomenon could be already occurring with the observed Cerro Prieto I enthalpy. If this is the case, then the predicted enthalpy would be a pessimistic value. Therefore, it would be worthwhile to continue generating this kind of data to verify such field behaviour.

Figure 17 compares the predicted pressure and enthalpy values to that of the steam-water saturation curve. As it can be observed, the Cerro Prieto I region remained single phase (liquid) during the predicted period.

CONCLUSIONS

1.- An acceptable pressure and enthalpy history match of the Cerro Prieto I region was obtained considering a steady-state recharge assumption, for the production period of 1973-1979.

2.- A 30 years predictive calculations using this coarse grid model indicate that reservoir pressure in this part of the field will slowly decrease to 96 bars. However, the reservoir enthalpy will continue to decline but a lower decline rate than at the begining of the field explotation.

3.- Because of the strong recharge taking place in this part of the field, the model predicts that Cerro Prieto I will not come into two phase conditions during the predicted period, under the proposed explotation program.

4.- The Cerro Prieto I predicted enthalpy of 1030 KJ/Kg (a liquid water temperature of 237 C) could be a rather pessimistic value. Further enthalpy data is needed to validate this conclusion.

5.- This coarse grid model suggests that the eventual demise of the Cerro Prieto I region would be a thermal degradation (i.e., cooling effect) rather than a pressure decline in the classical sense.

ACKNOWLEDGEMENTS

The authors would like to thank Coordinadora Ejecutiva de Cerro Prieto and also Instituto de Investigaciones Electricas for the opportunity given to them in presenting this paper.

REFERENCES

The following abbreviations will avoid monotonous repetitions:

CPI : Proceedings of the First Symposium on the Cerro Prieto Geothermal Field, September 20-22, 1978, San Diego, Ca.

CPII : Proceedings of the Second Symposium on the Cerro Prieto Geothermal Field, October 17-19, 1979, Mexicali, B. C., Mexico.

CPIII: Proceedings of the Third Symposium on the Cerro Prieto Geothermal Field, March 24-26, 1981, San Francisco, Ca.

CPIV : Proceedings of the Fourth Symposium on the Cerro Prieto Geothermal Field, August 10-12, 1982, Guadalajara, Jal., Mexico.

1.- Abril, G.A., Noble, J.E., (1978): "Correlaciones de Secciones Transversales en Base a Registros Eléctricos de Pozos del Campo Geotérmico de Cerro Prieto", CPI, pp. 41-46.

2.- Bermejo et. al. (1979): "Variación de la Presión en el Yacimiento de Cerro Prieto durante su Explotación", CPII, pp. 473-493.

3.- Castañeda, M., Abril, A.G., Arellano, V., Márquez, R.M., Sánchez, J.R. (1982): "Entrenamiento para el Desarrollo Sistemático de la Ingeniería de Yacimientos en el Campo Geotérmico de Cerro Prieto", Instituto de Investigaciones Eléctricas, Internal Report IIE/11/FE-G30/1678/I 01/P, Sept 1982.

4.- Castañeda, M., Márquez, R., Esquer, C.A., Arellano, V. (1983): "Entrenamiento para el Desarrollo Sistemático de la Ingeniería de Yacimientos en el Campo Geotérmico de Cerro Prieto", Instituto de Investigaciones Eléctricas, Internal Report IIE/11/1678/I 03/F.

5.- Coats, K.H., George, W.D., Chu, C., and Marcum, B.E. (1974): "Three Dimensional Simulation of Steam Flooding", Society of Petroleum Engineering Journal, Vol. 14, Number 6.

6.- Cobo, J.M. (1981): "Configuración de los Cuerpos Litológicos de Lodolita, Lutita Café, Lutita Gris, Zonas de Sílice y Epidota y sus Relaciones con la Tectónica del Campo Geotérmico de Cerro Prieto", CPIII, pp. 29-42.

7.- Domínguez, B. (1982): Perforación Geotérmica en Cerro Prieto", CPIV, pp. 217-232.

8.- Grant, M.A., Truesdell, A.H., Mañón, M. A. (1981): "Production Induced Boiling and Cold Water Entry in the Cerro Prieto Geothermal Reservoir Indicated by Chemical and Physical Measurements", CPIII, pp. 221-237.

9.- Grant, M.A., Sullivan, M.J. (1982): "The Old Field at Cerro Prieto considered as a Leaky Aquifer", CPIV, pp. 123-132.

10.- Lippman, M.J., Bodvarsson, G.S. (1982): "Modeling Studies on Cerro Prieto", CPIV.

11.- Minutes of the Second Cerro Prieto Internal DOE/CFE Workshop, Hotel Fiesta, San Felipe, B.C., Mexico, January 19-21, 1982.

12.- Programa de Obras e Inversiones del Sector Eléctrico, (POISE), Comisión Federal de Electricidad, Enero 1983.

13.- Rivera, R., Bermejo, F.J., Castillo, F., Pérez, H., Abrajan, A. (1982): "Actualización en el Estudio del Comportamiento y Distribución de Temperaturas en Cerro Prieto II y III", CPIV, pp. 93-112.

14.- Sánchez, R.J., De la Peña, L.A. (1981): "Geohidrología del Aquífero Geotérmico de Cerro Prieto", CPIII, pp. 309-323.

15.- Westwood, J.D. (1981): "The Application of Lumped Parameter Modeling to the Cerro Prieto Geothermal Field", Geothermal Resources Council Trans,, Vol. 5, June 1981.

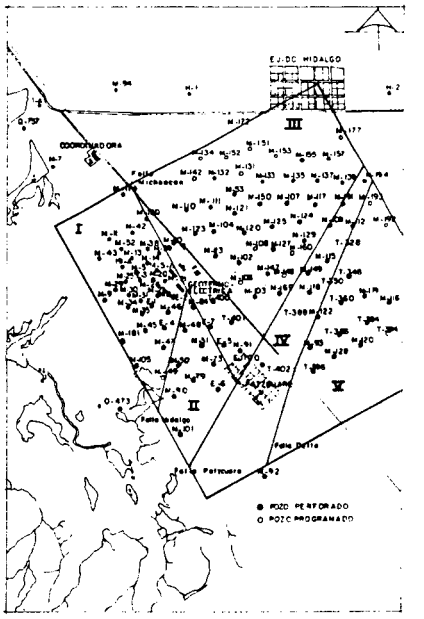

Fig. 1 Extended field area used in this work.

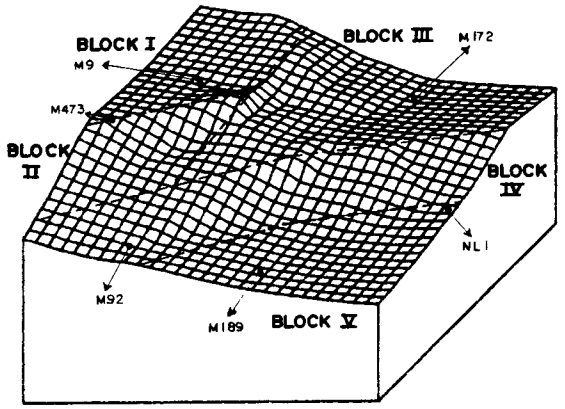

Fig. 2. Tridimensional representation of the top of the gray shale unit.

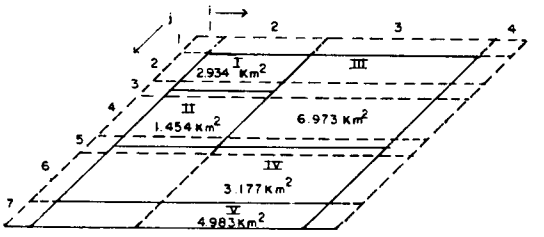

Fig. 3 . Schematic distribution of aereal grid elements.

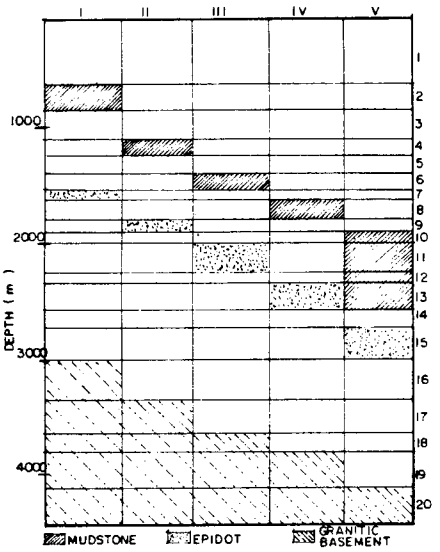

Fig. 4 . Vertical representation of the grid model.

PARAMETER \ UNIT	UNCONSOLIDATED SEDIMENTS	MUDSTONE	GRAY SHALE COFFE-COLORED SHALE	BIOTITE GRANITE
POROSITY (fraction)	0.10	0.04	0.1	0.02
HORIZONTAL PERMEABILITY (md)	100	1	50	0.1
VERTICAL PERMEABILITY (md)	20	5	10	0.01
THERMAL CONDUCTIVITY BTU/ft.°F	35.0	35.0	35.0	35.0
ROCK HEAT CAPACITY BTU/ft³-°F	39.5	39.5	39.5	39.5
ROCK COMPRESSIBILITY (psi^{-1})	4×10^{-6}	4×10^{-6}	4×10^{-6}	4×10^{-6}

Fig. 5 . Initial reservoir parameters for each model unit.

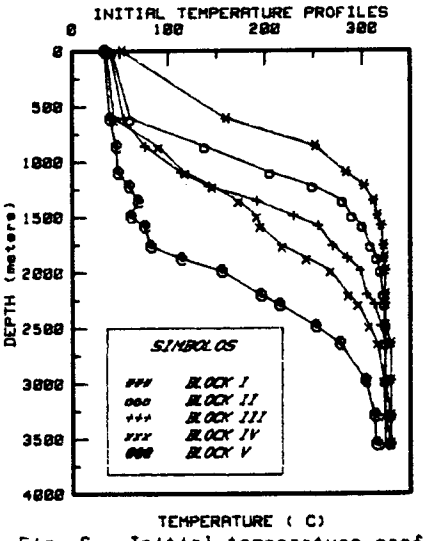

Fig. 6 . Initial temperature profile for each main block.

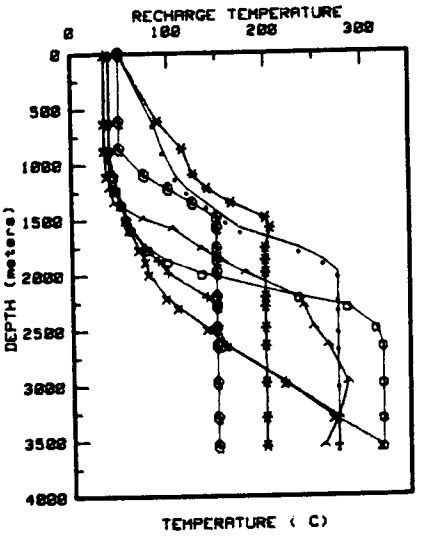

Fig. 7 . Recharge temperature profiles considered in this work.

MODEL WELL NUMBER	LOCATION I	J	K	WELL	BLOCK
1	2	2	2	M9, M291	I
2	2	2	4-5	M2911, M11, M31, M9A, M15A, M26, M27, M14, M5, M21A, M35, M8, M42.	I
3	2	2	5	M-20, M45, M25, M46, M39, M-30, M34, M43.	I
4	2	2	7		I
5	2	4	5	M48, M50, M90	II
6	2	4	5-7	M51,	II
7	2	4	10-11	M101	II
8	2	4	9	M84, M73, M79	II
9	3	2	11	M53, M91, M102, M103, M113, M117, M120, M121, M124, M125, M135, M137, M139, M150, M155, M157, M169, M177, M195, E5, E7.	III
10	3	2	9	M104, M110	III
11	2	4	13-14	E6	II
12	2	2	9	E2	I
13	3	2	12	M133, M127	III
14	3	2	13-14	M111	III
15	2	6	13	M109, M112, M115, M118, M122, M149, M191, M194, M328, M350 M388	IV
16	2	7	15	M93, M116, M119, M128, M348 M364, M366, M386, M395	V
17	3	4	11	M129, M147, T400	III

Fig. 8 . Location of the groups of wells in the coarse grid model.

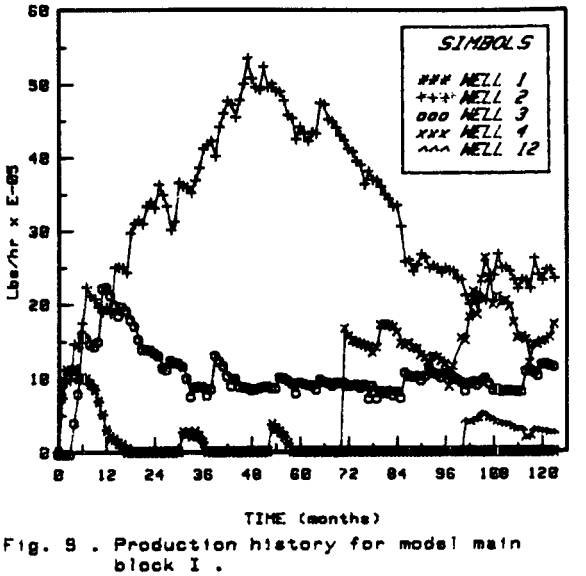

Fig. 9 . Production history for model main block I .

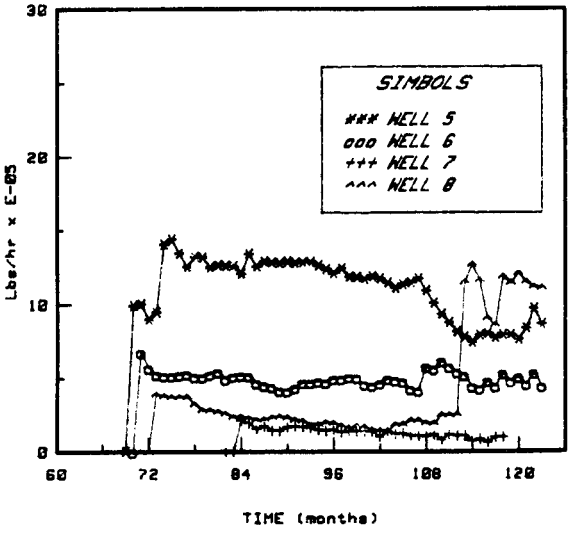

Fig. 10 . Production history for model main block II.

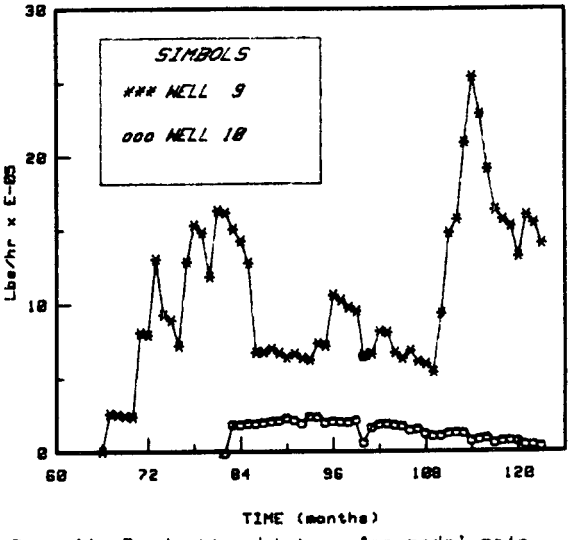

Fig. 11. Production history for model main block III.

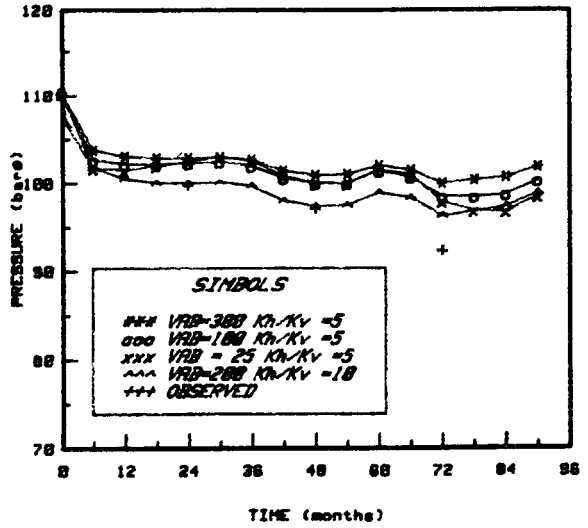

Fig. 12 . Simulated pressure for the initial reservoir parameters.

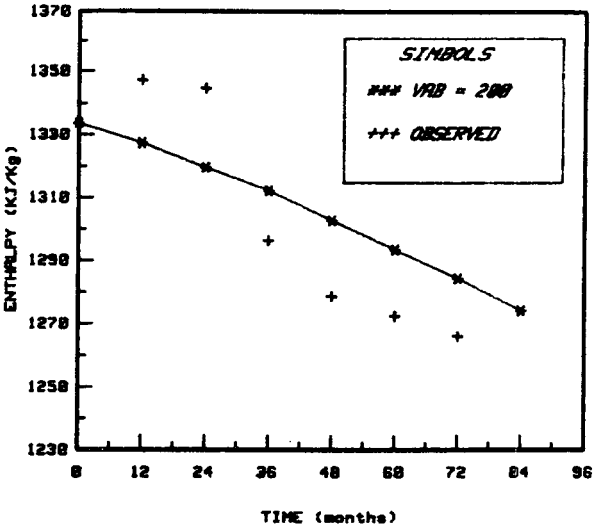

Fig. 13 . Simulated enthalpy for the case Kh/Kv = 10 , Kh = 50 md .

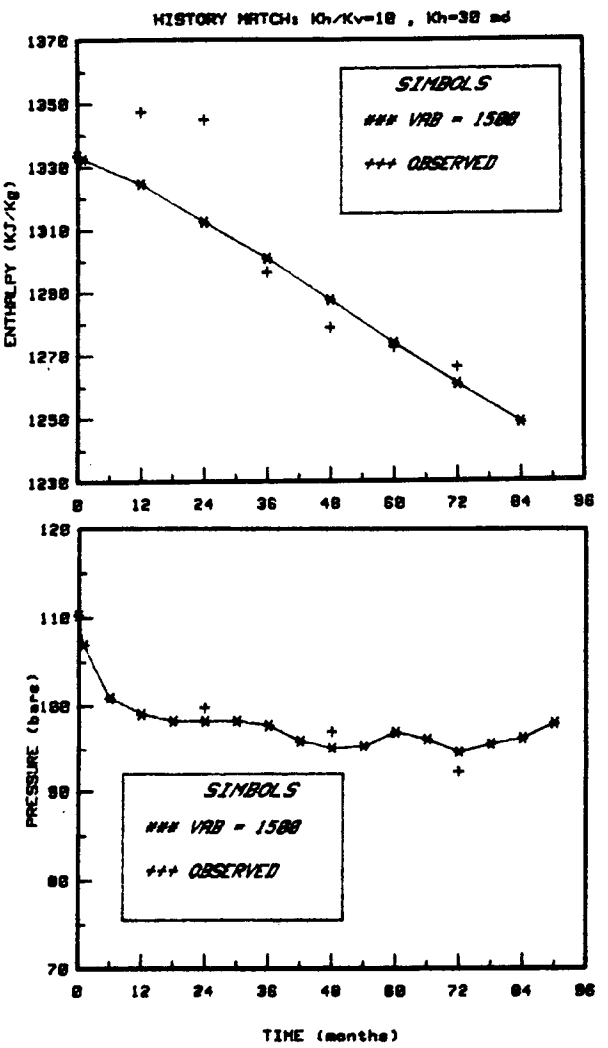

Fig. 14 . Pressure and enthalpy match for Cerro Prieto I (at depth of 1200 m)

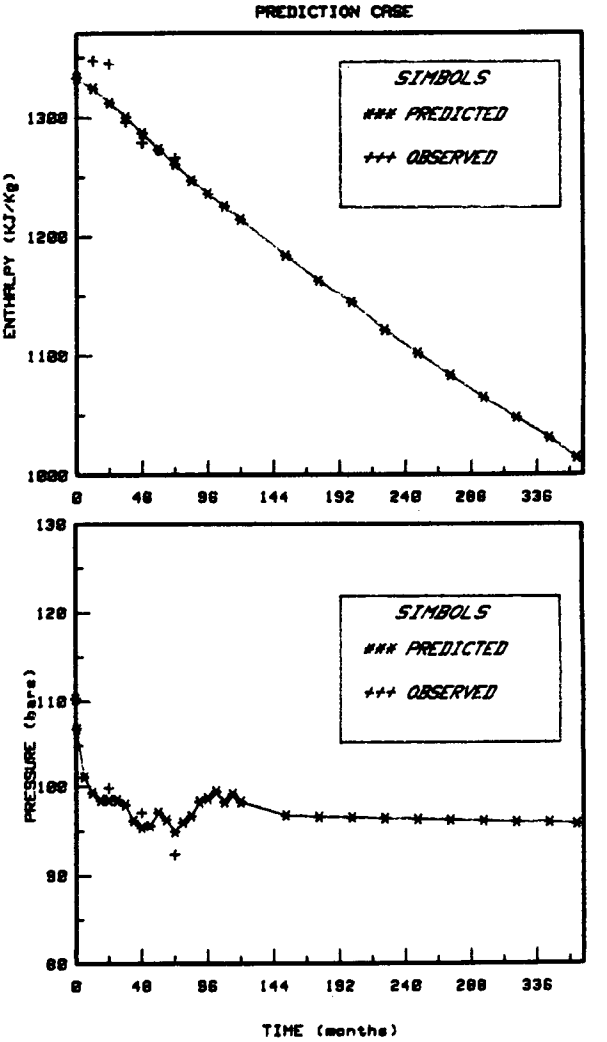

Fig. 16 . Predicted pressure and enthalpy for Cerro Prieto I region (period 1973-2003)

POWER PLANT	UNIT	DATE	WELLS	MASS RATE PER WELL (Ton/hr.)
CP II	1	DIC/1/83	M93, M116, M119, M128, M364, M366, M386, M395, M348, M122 T400.	233.1
	2	NOV/1/84	M129, M147, M27, M115, M118, M149, M328, M350, M388.	233.1
CP III	1	ENE/1/85	M150, M117, M121, M113, M124, M110, M109, M112, M125, M111.	233.1
	2	JUL/1/85	M135, M137, M139, M157, M155, M177, M195, M191, M194, M133.	233.1

Fig. 15. Required mass flow rate and approximated starting operation dates for the two new power plants.

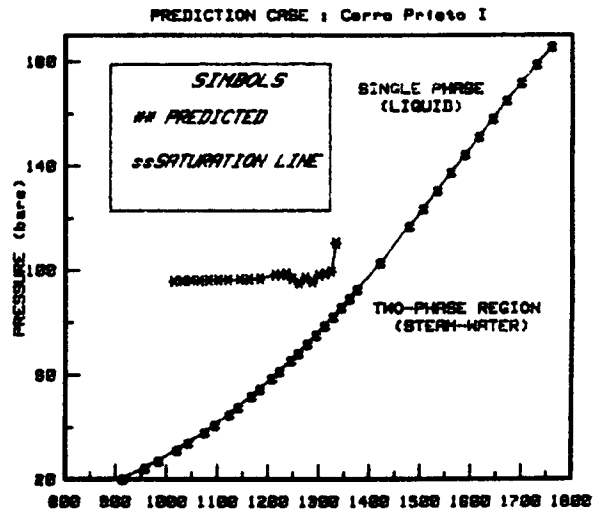

Fig. 17 . Comparison of predicted pressure and enthalpy with the steam-water saturation curve values